Appl Petrochem Res (2016) 6:269–277
DOI 10.1007/s13203-016-0159-9

ORIGINAL ARTICLE

Catalytic decomposition of carbon-based liquid-phase chemical hydrogen storage materials for hydrogen generation under mild conditions

Felipe Sánchez[1] · Davide Motta[1] · Nikolaos Dimitratos[1]

Received: 24 January 2016 / Accepted: 24 May 2016 / Published online: 4 June 2016

Abstract The increasing demand of energy requires the development of sufficient and sustainable energy sources. However, the upcoming hydrogen economy is suffering from challenges which need to be solved. In this context, the search for liquid hydrogen storage materials and successful utilisation is crucial due to the high gravimetric and volumetric hydrogen densities, easy recharging, low capital investment, and low potential risks. In this review, we survey the progress made in hydrogen generation from carbon-based liquid-phase chemical hydrogen storage materials, focusing mainly on the catalytic decomposition of formic acid for hydrogen production.

Keywords Formic acid decomposition · Hydrogen generation · Supported metal nanoparticles · Colloidal methods

Introduction

The everyday increasing energy consumption is forcing the exploration of alternative energy strategies to fulfil the currently rising requirements without further damage to the environment [1, 2]. The installation of a sustainable energy supply chain is one of the greatest challenges to be addressed in this century [3, 4]. Compared with the conventional combustion engines, fuel cells have a higher fuel conversion and electrical efficiency producing additionally less toxic emissions [3, 5]. These factors and the lower greenhouse gas emissions, low noise levels, and high fuel utilisation rates have converted, in the last few years, fuel cells to an attractive alternative for portable devices and transport with significant long term economic and environmental benefits [6–9]. On the other hand, the high cost, life time issues, and, more importantly, the availability of economically profitable hydrogen generation, transportation, and storage technologies are the main drawbacks that limit the commercialisation of fuel cells [2, 5, 9, 10].

Advantages and drawbacks of hydrogen as energy carrier

Hydrogen, with a high energy density of 120 kJ g^{-1}, is an environmentally benign fuel, in which water is the only product of its reaction with oxygen [11]. Hydrogen, the most abundant element in nature, is, as well, the most versatile fuel due to the fact that it can be converted to other forms of energy as electricity through electrochemical processes, to heat through catalytic combustion, or to heat source through various chemicals reactions [12]. Hence, energy systems powered by hydrogen seem to be an attractive alternative to the current fuel-based energy systems. However, despite the potential of the use of hydrogen, its widespread use as a major energy carrier is currently limited by the capacity limitations of hydrogen storage technologies and by the safety issues related with its storage and transportation under mild conditions [13].

Some of those issues are the high flammability in the presence of oxygen and the traditional physical storage methods using high pressure gas cylinders of up to 800 bar changing its state conditions (pressure, temperature, and phase). This requires energy intensive processing and has safety risks making public acceptance difficult, besides the

✉ Nikolaos Dimitratos
sacnd1@cardiff.ac.uk

[1] School of Chemistry, Cardiff University, Main Building, Park Place, Cardiff CF10 3AT, UK

significant weight and volume requirements. To solve this problem, during the last two decades, great scientific efforts have been made. The current research is exploring new methods to store or produce hydrogen under more favourable temperatures and pressures.

Over the last decades, alternatives to physical hydrogen storage have been researched. These new methods can be classified as physisorption materials and chemical release systems. In the former method, hydrogen is adsorbed into a porous network, such as zeolites [14], MOFs [15], clathrate hydrates [16], various carbon materials [14], and conventional organic polymers [17]. In the latter, a hydrogen-rich material is subjected to a decomposition process, which is preferably reversible. First, due to several advantages as stability and safety, much attention was paid to solid-state hydrogen storage materials [18, 19]. Possible solid-phase systems include metal and non-metal hydrides [20], amines [21], amides [22], and ammonia-like complexes [23]. However, despite these features, it presents important drawbacks as the high temperature necessary to desorb hydrogen or the slow hydrogen release kinetics. Due to this, liquid-phase hydrogen storage materials as *N*-ethylperhydrocarbazole [24], alcohols [25], or formic acid have been recently investigated. We will focus our attention in liquid carbon-based hydrogen carriers.

Catalytic decomposition of alcohols

Methanol is a suitable material to store and handle hydrogen due to the following aspects: is liquid a room temperature which favour the storage and delivery; methanol has a 12.6 wt% hydrogen content; it can be produced industrially from biomass on a large scale; it does not have C–C bond; therefore, less coke is produced during its reaction. Different thermochemical methods can be used to produce hydrogen from methanol. Those methods are steam reforming, direct decomposition, autothermal reforming, and partial oxidation. Methanol steam reforming [26] is a well-known process which has attracted attention in energy generation using indirect methanol fuel cells [27]. It takes place at high temperatures (200–300 °C) and pressures (25–50 bar). This and the fact that the distribution of products is too wide are the main drawbacks.

Beller et al. studied the dehydrogenation of methanol using ruthenium pincer complexes in methanolic sodium hydroxide [28], achieving a TOF of 4719 h^{-1}, showing a higher selectivity and reaction rates [29] if compared with the previous methods and mainly producing hydrogen and carbon dioxide in the form of carbonate. Examples of selective dehydrogenation of methanol and formic acid with a ruthenium pincer complex are also described by Grutzmacher et al. [30]. However, the development of a suitable catalyst for methanol dehydrogenation at low temperature is still necessary, since, as stated before, an important application for these catalysts could be fuel cells in portable devices.

Other alcohols, such as ethanol, have also been studied as a hydrogen carrier. Compared with methanol, ethanol is a non-toxic fuel, inexpensive, and moreover, in countries, such as USA and Brazil, the infrastructure required for ethanol production and distribution is already established, since ethanol is currently distributed. Those factors have made ethanol an economically and environmentally attractive fuel. Moreover, the content of hydrogen is slightly higher (13.1 wt%) compared with methanol.

Back in the 1970s, several studies were carried out in the dehydrogenation of ethanol among other alcohols using homogeneous catalysts. The decomposition of ethanol by rhodium–tin chloride catalysts in acidic media was first studied by Charman et al. [31]. Idriss et al. studied the heterogeneous photo-catalytic dehydrogenation of ethanol using titania doped with gold, however, obtaining a poor TOF [32]. Beller et al. also described the dehydrogenation of ethanol to ethyl acetate and acetaldehyde using a ruthenium pincer complex at an initial TOF of 1483 h^{-1} [33].

Catalytic decomposition of formic acid

Recently, formic acid, a major product formed during biomass processing, has been studied as a safe and convenient hydrogen storage material due to its high volumetric hydrogen content, liquid state at room temperature, high stability, environmental benignity, and non-toxicity, and the fact that can produce only gaseous products (H_2/CO_2) by decomposition [34]. Formic acid has gravimetric hydrogen capacity of 4.4 wt%. Hydrogen stored in formic acid decomposition can be released via a catalytic dehydrogenation reaction (Eq. 1); however, the undesirable dehydration reaction (Eq. 2) can likewise occur depending on reaction conditions and choice of catalysts. Dehydration usually is promoted by heating and acidity. Selective dehydrogenation is indispensable for the production of ultrapure H_2 without dehydration, since toxic CO contamination produced by the latter pathway is not tolerated by fuel cells.

$$\mathrm{HCOOH} \rightarrow \mathrm{CO_2} + \mathrm{H_2} \quad \Delta G = -48.4\ \mathrm{kJ\,mol^{-1}} \tag{1}$$

$$\mathrm{HCOOH} \rightarrow \mathrm{CO_2} + \mathrm{H_2O} \quad \Delta G = -28.5\ \mathrm{kJ\,mol^{-1}}\,. \tag{2}$$

To close the cycle (Fig. 1), CO_2 can be hydrogenated back to formic acid resulting in a CO_2 neutral process with a high selectivity and high catalytic activity [35].

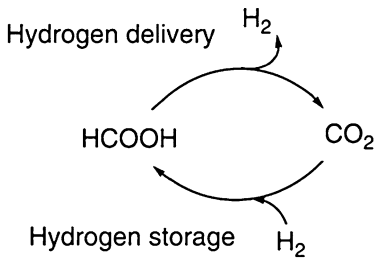

Fig. 1 Formic acid/carbon dioxide cycle for hydrogen storage

Formic acid has intensely been investigated for hydrogen generation by either homogeneous or heterogeneous catalytically decomposition approaches. There are reports of effective decomposition of formic acid using homogeneous catalysts at ambient temperatures, and recently, the catalytic efficiency has been significantly improved [36–39].

Homogeneous catalytic decomposition of formic acid

At high temperatures as 120 °C, a TOF of 18,000 h^{-1} was achieved at 120 °C using $[Rh_2(HCO_2)_2(CO)_4]$ [40]. If we focus in the main important results at mild conditions, Fukuzumi et al. reported a TOF of 426 h^{-1} at room temperature, using a heteronuclear iridium-ruthenium complex $[Ir(Cp^*)(H_2O)(bpm)Ru(bpy)_2]^{4+}$ in the presence of sodium formate [41]. However, they reached a higher TOF of 1880 h^{-1} when they prepared a cyclometalated organoiridium complex $[Ir(Cp^*)(pba)(H_2O)]^+$ based on 4-(1H-pyrazol-1-yl)benzoic acid (pba) in a potassium formate system [42]. At slightly higher temperature, 40 °C, Beller et al. studied several homogeneous catalysts in the presence of amines. An initial TOF of 3630 h^{-1} was reached using a ruthenium phosphine catalyst $RuBr_3{\cdot}xH_2O$/$3PPh_3$ in a 5HCOOH-2Net_3 mixture [43], while, with $[RuCl_2(PPh_3)_3]$ and dimethylformamide, the TOF reached 2688 h^{-1} [37]. They made a remarkable discovery when they found that the hydrogen generation from formic acid using ruthenium-based catalysts could be improved by the utilisation of visible light [39]. All those previous results are noteworthy; however, the separation of the catalyst from the reaction mixture, harsh reaction conditions, poor selectivity, and the need for organic solvents/additives prevent formic acid decomposition using homogeneous catalysts from scaling-up for industrial applications. The facile control of hydrogen generation using heterogeneous catalysts is an attractive approach [44, 45].

Heterogeneous catalytic decomposition of formic acid

There have been some studies performed in the gas phase catalytic decomposition of formic acid, requiring, therefore, the introduction of inert carrier gas to dilute formic acid below its saturated vapour pressure, using a vacuum environment or increasing temperatures to at least 100 °C [46]. In these conditions, Bulushev et al. reached a TOF of 255 h^{-1} at 100 °C using 1 wt% Pd/C [47].

Due to those previously mentioned drawbacks and the selectivity obtained limits the utilisation of these processes for fuel cells applications. To utilise hydrogen in a fuel cell in portable devices, it is necessary to develop heterogeneous catalysts for liquid-phase formic acid decomposition under mild conditions. Table 1 presents several heterogeneous catalysts for formic acid decomposition at mild conditions. The first studies on the formic acid heterogeneous catalytic decomposition using Pd–Au alloy wires started in 1957 [48], and it was followed by studies using Pd/C (1 wt% Pd) at room temperature [49]. A high TOF of 820 h^{-1} was recently reported using Pd and Pd–Ag nanoparticles combined with weakly basic resin bearing amino groups at 75 °C and using a solution of formic acid and sodium formate 9:1. The authors reported a maximum rate of reaction of 2880 ml min^{-1} g^{-1} [50]. Xing et al. developed Pd–Au and Pd–Ag alloyed nanoparticles supported on carbon and overcame the poisoning effect by CO by-product of the decomposition of formic acid at low temperatures. The authors reported that the activities of Pd–Au/C and Pd–Ag/C can be enhanced by co-deposition with CeO_2 giving a TON of 227 and 76 h^{-1}, respectively, at 92 °C as presented in Fig. 2 [51]. However, following the requirement of mild conditions, to use the fuel cell in portable devices, we will focus in the main results obtained at low temperatures.

Chan et al. studied the performance of Pd/C toward formic acid decomposition at temperatures between 21 and 60 °C and using formic acid concentrations between 1.33 and 5.33 M showing that the order of reaction to formic acid decreases with the increasing of the temperature from 0.51 to 0.37 [52]. Jiang and co-workers synthesised in situ Pd/C in the presence of citric acid, this catalyst displayed a TOF of 64 h^{-1} after 160 min even at 25 °C, higher than the 16 h^{-1} obtained in the absence of citric acid. This behaviour has been related to the formation of smaller particles with higher accessibility of the surface of the NPs prepared in the presence of citric acid compared with the ones prepared with other dispersing agent, such as polyvinyl pyrrolidone or ascorbic acid [53]. However, it has been shown that the majority of Pd/C

Table 1 Supported metal nanoparticles for catalytic formic acid decomposition at mild conditions

Catalyst	*T* (°C)	Reagent	TOF (h^{-1})		Activation energy (KJ mol^{-1})	Refs.
			Initial	2 h		
Pd/C	21	Formic acid (1.33 M)	18	15[a]	53.7	[52]
	30		48	28[a]		
Pd/C (citric acid)	25	Formic acid		64[b]		[53]
Pd/C	30	Formic acid: Sodium formate 1:9		228.3		[54]
Pd/C	50	Formic acid (1 M)	30			[56]
Au/C	50	Formic acid (1 M)	80			
$Au_{41}Pd_{59}$/C	50	Formic acid (1 M)	230		28 ± 2	
Ag@Pd (1:1)	20	Formic acid		125[c]		[57]
	35			156[c]	30	
	50			252[c]		
Ag/Pd alloy (1:1)	20			144[c]		
$Ag_{42}Pd_{58}$	50	Formic acid (1 M)	382		22 ± 1	[58]
Pd-MnO_x/SiO_2-NH_2	20	Formic acid (0.265 M)	140		61.9	[59]
	50		1300			
Au/ZrO_2	50	Formic acid	1590			[61]
$Ag_{0.1}Pd_{0.9}$/rGO	25	Formic acid	105			[62]
$Co_{0.30}Au_{0.35}Pd_{0.35}$	25	Formic acid	80			[64]
$Ni_{0.40}Au_{0.15}Pd_{0.45}$/C	25	Formic acid	12			[65]

[a] TOF values calculated after 50 min

[b] TOF values calculated after 160 min

[c] TOF values calculated based on the surface metal sites

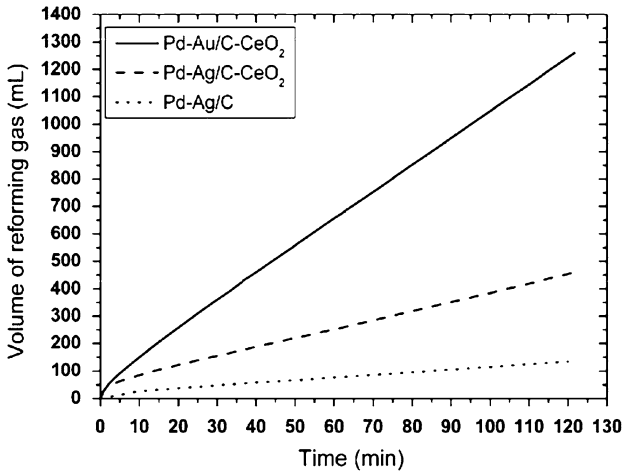

Fig. 2 Volume of gas produced at 365 K with 5.00-ml 9.94-M formic acid–3.33-M sodium formate solution. Reprinted with permission from Ref. [51]. Copyright (2008) Royal Society of Chemistry

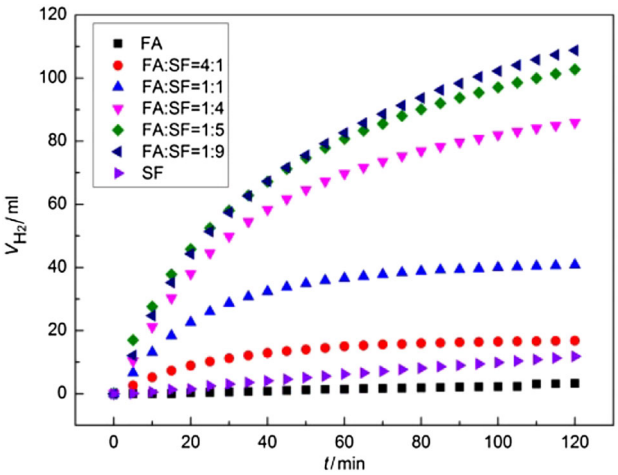

Fig. 3 H_2 volume produced for the catalysed decomposition of FA-SF systems for different FA-SF ratios. Reprinted with permission from Ref. [54]. Copyright (2014) Elsevier

catalysts deactivate quickly due to the poisoning intermediates, resulting in its failing in applications [47]. Nevertheless this issue, Zhang et al. studied the effect that the ratio formic acid/sodium formate has in the hydrogen volume generated, reaching a maximum TOF of 228.3 h^{-1} at 30 °C after 2 h using a solution of formic acid and sodium formate 1:9, respectively [54]. The mechanism proposed for the decomposition of sodium formate does not produce CO, unlike the decomposition of pure formic acid under certain conditions. Figure 3 shows the effect of the ratio formic acid/sodium formate on the hydrogen volume produced.

An important discovery was made by Ojeda and Iglesia. They reported that the activity of a gold catalyst supported over Al_2O_3 was much higher than that of Pt, likely due to the size of the gold domains. In this work, they have also investigated the mechanism of reaction on the Au/Al_2O_3 and Pt/Al_2O_3 using kinetic isotope effect (KIE). This kinetic test consists in the use of different deuterium substituted substrates, such as HCOOD, DCOOH, and DCOOD, to distinguish between different reaction pathways. The exclusive formation of HD using both HCOOD and DCOOH indicates that the absorbed H atoms from –OH to –CH bond recombine together, and desorption is an irreversible step. KIE values (r_H/r_D) for HCOOD were 1.1 and 1.6 for Pt and Au, respectively, where for DCOOH, KIE values were 1.7 and 2.5, and finally, for DCOOD, KIE were 2.1 and 4.7. These values suggest the dissociation of O–H as the first step, almost thermodynamic in the case of Pt. The H adsorption is followed by the reaction between H atom and C–H bond of formates to form of H_2 and CO_2 [55].

Sun et al. compared the formic acid decomposition using monometallic Pd/C, Au/C, and bimetallic alloys with different Au–Pd atomic compositions. They obtained the highest activity with an alloy C-$Au_{41}Pd_{59}$ catalyst, reaching an initial TOF of 230 h^{-1} at 50 °C with an apparent activation energy as low as 28 kJ mol^{-1}. The monometallic counterparts presented a much lower activity, being the TOF for Pd/C, 30 h^{-1}, and, for Au/C, 80 h^{-1}, all at the same conditions [56]. This result shows that bimetallic nanoparticles can promote the catalytic activity and selectivity for formic acid dehydrogenation compared to the monometallic species. Since the catalytic activities are dependent on the catalyst surfaces, these can be modified by adding a different metal or changing the morphology. They explained this enhancement by the fact that an alloy of Au and Pd can moderate the formic acid adsorption and activation during the reaction. Figure 4a presents the volumetric gas amount ($CO_2 + H_2$) versus time for the following catalysts: Pd/C, Au/C, and C-$Au_{41}Pd_{59}$, showing the enhancement on formic acid dehydrogenation by the bimetallic catalyst. Figure 4b displays the TEM of the $Au_{41}Pd_{59}$ NPs. These nanoparticles present a mean particle size of 4 ± 0.2 nm diameter. Figure 4c shows the X-ray diffraction (XRD) patterns of the Au, Pd, and $Au_{41}Pd_{59}$ NPs synthesised, demonstrating the formation of the alloy structure due to the presence of diffraction peaks in between those of Au and Pd.

Tsang et al. developed Ag–Pd core–shell nanoparticles (diameter 8 nm) with the thinnest continuous Pd shell and supported on carbon-based materials obtaining a TOF (based on the surface Pd site over the Ag core–Pd shell) of 125 h^{-1} at 20 °C and 252 h^{-1} at 50 °C with a reported activation energy of 30 kJ mol^{-1}, one of the lowest reported in the current literature. Figure 5a illustrates the comparison between Ag–Pd core–shell (Ag@Pd), Ag–Pd alloy, and pure Pd displaying the higher activity of the core–shell structure related to a larger promoting effect of the core metal than in the case of the alloy structure displayed by higher TOF in function of moles of Pd used and for both larger than the TOF of the monometallic catalyst, still insufficient for practical application. When increasing the temperature above 50 °C, CO was detected in inappropriate concentrations for fuel cells, above 10 ppm. Pure Pd and Ag/Pd alloy were studied and a higher TOF was produced with the alloy, nevertheless, the poorer volume of hydrogen produced prevents this catalyst to be cost-effectively used. Figure 5b presents the core–shell structure of a Ag@Pd nanoparticle synthesised in this work characterised using atom probe tomography (APT); this image clearly shows how the best performance catalyst with a Pd:Ag

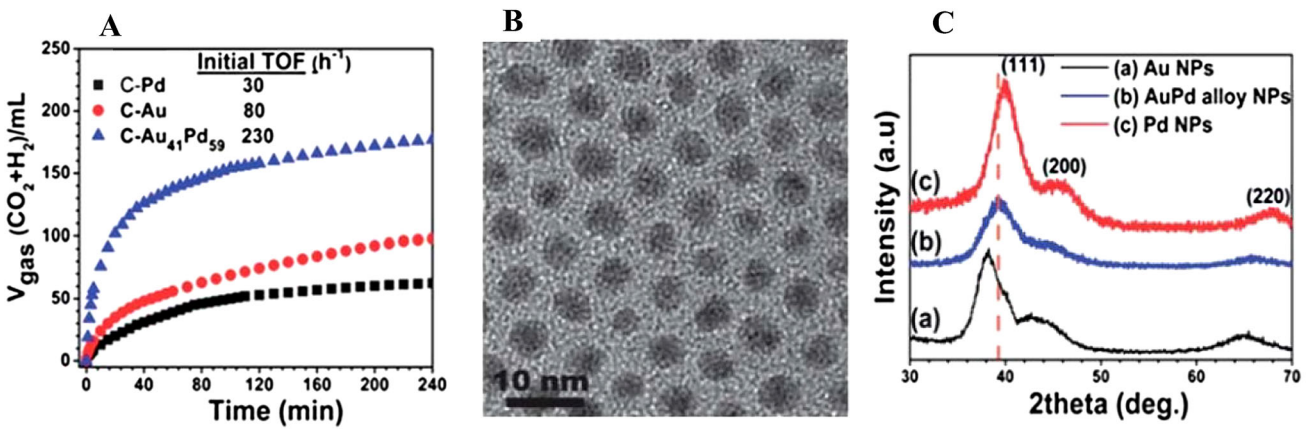

Fig. 4 **a** $CO_2 + H_2$ volume vs. time for Pd/C, Au/C, and C-$Au_{41}Pd_{59}$, **b** TEM image of the prepared $Au_{41}Pd_{59}$ NPs, **c** XRD patterns of the Au, Pd, and $Au_{41}Pd_{59}$ NPs. Reprinted with permission from Ref. [56]. Copyright (2013) Royal Society of Chemistry

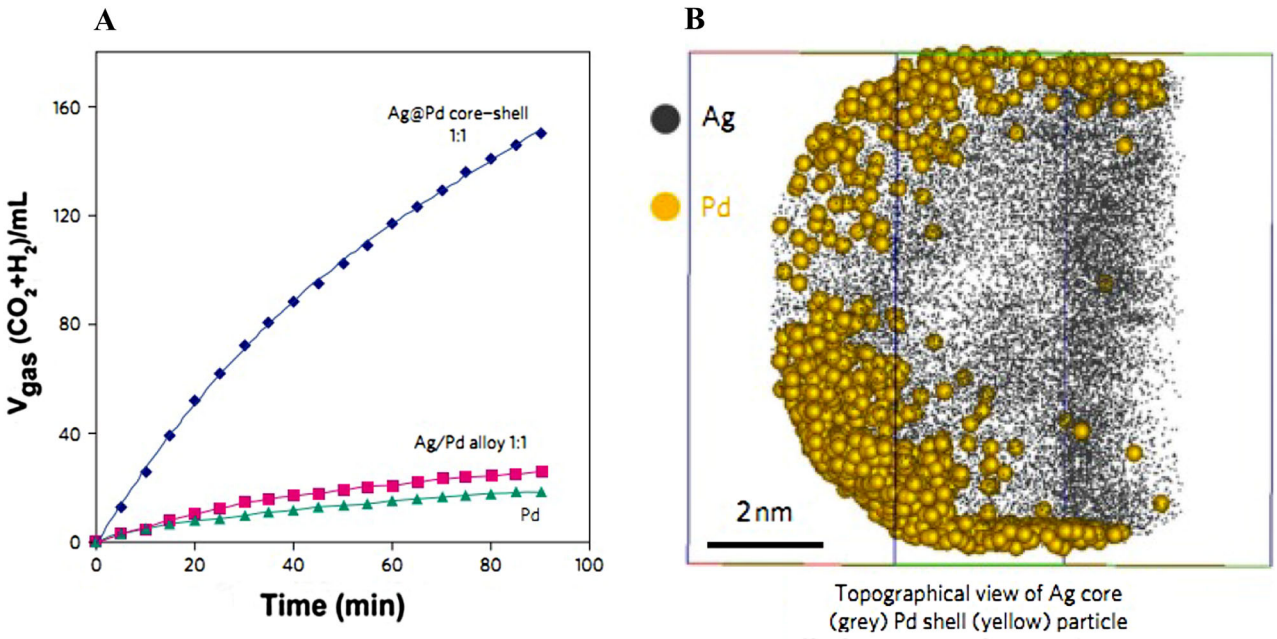

Fig. 5 **a** $CO_2 + H_2$ volume vs. time for Ag@Pd, Ag-Pd alloy, and Pd catalysts, **b** ATP data: atom map of a Ag@Pd nanoparticle. Reprinted with permission from Ref. [57]. Copyright (2011) Nature

ratio of 1:1 is formed by a continuous single layer of Pd, in this condition strain of the active surface, and electronic effect due to the core metal is optimised [57].

Sun and co-workers reported a composition-controlled synthesis of monodisperse 2.2 nm highly active and durable Ag–Pd NPs. They studied the composition-dependent catalysis and found that the $Ag_{42}Pd_{58}$ NPs have the highest activity of those studied with an initial TOF of 382 h^{-1} and an apparent activation energy of 22 ± 1 kJ mol^{-1} [58]. Recently, Zahmakiran et al. synthesised a bimetallic Pd-MnO_x NPs supported on 3-aminopropyl functionalised silica (Pd-MnO_x/SiO_2-NH_2) providing a very high activity (TOF = 1300 h^{-1} at 50 °C) at high conversion (>99 %) and selectivity (>99 %). The reported values are among the best heterogeneous catalysts reported in the additive-free dehydrogenation of formic acid under mild conditions [59]. One of the highest TOF values reported was achieved by Xu and co-workers. They synthesised stable Pd NPs on nanoporous carbon MSC-30 and produced formic acid decomposition with a TOF of 2623 h^{-1} at 50 °C and 750 h^{-1} at 25 °C, without undesired CO formation. This performance has been related to the small particles size, 2.3 ± 0.4 nm, obtained adding NaOH before the reduction step in the deposition method and to the confinement of the NPs inside the porous structure of the carbon support. The activity of the Pd/MSC-30 is higher than the one exhibited by other Pd on porous C with similar particle size; thus, stronger metal-support interaction is present in the case of MSC-30 [60].

Cao and co-workers reported for the first time, the formic acid–amine mixture dehydrogenation using Au subnanoclusters (∼1.8 nm) dispersed on ZrO_2. The reaction proceeded efficiently and selectively, reaching a high TOF of 1590 h^{-1} at 50 °C [61]. In this study, the authors foresee a new generation of advanced nanocatalysts produced by tuning the Au clusters at the subnano level.

Reduced graphene oxide has been used as a single-layer carbon substrate to anchor metal NPs. Graphene has become a promising candidate as a substrate due to several properties, such as the high theoretical surface area (2600 m^2 g^{-1}) and conductivity, and low cost, among others. This unusual surface area produces a great dispersion which, moreover, added to the strong metal-support interaction, makes these catalysts resistant to aggregation. Yan et al. reported a facile method to synthesise Ag-Pd NPs assembled on reduced graphene oxide achieving a maximum TOF of 105 h^{-1} for the formic acid decomposition using $Ag_{0.1}Pd_{0.9}$/rGO at 25 °C reaching a 100 % H_2 selectivity [62].

As well as noble metals, there are studies reporting heterogeneous catalysts composed by the first-row transition metals. Being those resistant to acid corrosion when alloying with noble metals [63], cheaper and generally more easily available transition metals are good alternatives to noble metals. A trimetallic $Co_{0.30}Au_{0.35}Pd_{0.35}$ nanocatalyst prepared by Yan and co-workers reported an initial TOF of 80 h^{-1} at 25 °C which is an improved catalytic activity compared with the monometallic and

bimetallic counterparts [64]. The same group prepared as well $Ni_{0.40}Au_{0.15}Pd_{0.45}/C$, but obtaining a low TOF of 12 h^{-1} at 25 °C [65]. Zhang and co-workers, after further study of those transition metals, found that in some cases, Ni was eroded by H^+ resulting in the loss of activity; however, a possible solution to this problem could be the construction of a core–shell nanostructure, being the core the transition metal, improving, therefore, the activity and stability of the catalyst [66].

Conclusions and perspective

In this brief review, we have mentioned some recent developments toward hydrogen generation for applications in portable devices fuel cells. We have focused on the carbon-based liquid hydrogen carriers (methanol and formic acid) with a high potential in the near future. Despite in the last years, all these research efforts have improved the temperature, in which hydrogen is generated and the reaction kinetics; however, for practical applications in portable electric devices, there are still a few limitations to be addressed to establish a safe and efficient storage and delivery of hydrogen, so as to develop a sustainable hydrogen economy. Formic acid has increased the attention in the last few years due to the merits, it presents compared to others liquid hydrogen carriers. A cyclic system based on the formation and dehydrogenation of formic acid could be used as a power supply.

Research is currently being conducted to find catalysts with applications in fuel cells. To overcome the limitations above mentioned, the main requirements, these catalysts must fulfil, are to present a high activity at ambient temperatures and atmospheric pressure, near 100 % H_2 selectivity, reduced cost, good stability, and to convert the maximum amount of substrate with the minimum possible catalyst used.

It is evident from the current literature that a significant progress has been made toward the utilisation of formic acid as a promising liquid hydrogen carrier and the utilisation of supported bimetallic and trimetallic nanoparticles with alloyed structure, and small particle size (2–5 nm) shows to improve issues regarding improvement activity, selectivity, and stability. However, more systematic studies are needed for understanding and correlating structure–activity relationships and unravelling reaction pathways. In situ/operando studies and studying deactivation phenomena will lead to the design and synthesis of better and more efficient catalysts in this promising research area.

References

1. Sharma S, Ghoshal SK (2014) Hydrogen the future transportation fuel: from production to applications. Renew Sustain Energy Rev 43:1151–1158
2. Zhu Y, Ha SY, Masel RI (2004) High power density direct formic acid fuel cells. J Power Sources 130:8–14
3. Ren Y, Chia GH, Gao Z (2013) Metal-organic frameworks in fuel cell technologies. Nano Today 8:577–597
4. Afif A, Radenahmad N, Cheok Q, Shams S, Kim JH, Azad AK (2016) Ammonia-fed fuel cells: a comprehensive review. Renew Sustain Energy Rev 60:822–835
5. Kendall K, Pollet BG (2012) Hydrogen and fuel cells in transport, vol 4. Elsevier Ltd, Amsterdam
6. Larminie J, Dicks A (2003) Fuel cell systems explained, 2nd edn. Wiley, West Sussex
7. Wu HW (2016) A review of recent development: transport and performance modeling of PEM fuel cells. Appl Energy 165:81–106
8. Ugurlu A, Oztuna S (2015) A comparative analysis study of alternative energy sources for automobiles. Int J Hydrog Energy 40:11178–11188
9. Baroutaji A, Carton JG, Sajjia M, Olabi AG (2016) Materials in PEM fuel cells. Ref Modul Mater Sci Mater Eng 1–11. doi:10.1016/B978-0-12-803581-8.04006-6
10. Mandal K, Bhattacharjee D, Dasgupta S (2015) Synthesis of nanoporous PdAg nanoalloy for hydrogen generation from formic acid at room temperature. Int J Hydrog Energy 40:4786–4793
11. Park S, Vohs JM, Gorte RJ (2000) Direct oxidation of hydrocarbons in a solid-oxide fuel cell. Nature 404:265–267
12. Veziroglu TN, Sahin S (2008) 21st Century's energy: hydrogen energy system. Energy Convers Manag 49:1820–1831
13. Baykara SZ (2005) Hydrogen as fuel: a critical technology. Int J Hydrog Energy 30:545–553
14. Yang ZX, Xia YD, Mokaya R (2007) Enhanced hydrogen storage capacity of high surface area zeolite-like carbon materials. J Am Chem Soc 129:1673–1679
15. Dai H, Xia B, Wen L, Du C, Su J, Luo W, Cheng G (2015) Synergistic catalysis of AgPd@ZIF-8 on dehydrogenation of formic acid. Appl Catal B Environ 165:57–62
16. Veluswamy H, Kumar R, Linga P (2014) Hydrogen storage in clathrate hydrates: current state of the art and future directions. Appl Energy 122:112–132
17. Furukawa H, Yaghi OM (2009) Storage of hydrogen, methane, and carbon dioxide in highly porous covalent organic frameworks for clean energy applications. J Am Chem Soc 131:8875–8883
18. Lundin C, Lynch FE (1976) From gov. rep. announce. Index (USA) 76:99
19. Bogdanovic B, Schwickardi M (1997) Ti-doped alkali metal aluminium hydrides as potential novel reversible hydrogen storage materials. J Alloys Compd 253–254:1–9
20. Graetz J (2009) New approaches to hydrogen storage. Chem Soc Rev 38:73–82
21. Shen J, Yang L, Hu K, Luo W, Cheng G (2015) Rh nanoparticles supported on graphene as efficient catalyst for hydrolytic dehydrogenation of amine boranes for chemical hydrogen storage. Int J Hydrog Energy 40(2):1062–1070

22. Nakamori Y, Kitahara G, Ninomiya A, Aoki M, Noritake T, Towata S, Orimo S (2005) Guidelines for developing amide-based hydrogen storage materials. Mater Trans 46(9):2093–2097
23. Lu Z, Jiang H, Yadav M, Aranishiab K, Xu Q (2012) Synergistic catalysis of Au-Co@SiO_2 nanospheres in hydrolytic dehydrogenation of ammonia borane for chemical hydrogen storage. J Mater Chem 22:5065–5071
24. Wang Z, Tonks I, Belli J, Jensen CM (2009) Dehydrogenation of N-ethyl perhydrocarbazole catalyzed by PCP pincer iridium complexes: evaluation of a homogenous hydrogen storage system. J Organomet Chem 694:2854–2857
25. Iulianelli A, Ribeirinha P, Mendes A, Basile A (2014) Methanol steam reforming for hydrogen generation via conventional and membrane reactors: a review. Renew Sustain Energy Rev 29:355–368
26. Chin YH, Dagle R, Hu J, Dohnalkova AC, Wang Y (2002) Steam reforming of methanol over highly active Pd/ZnO catalyst. Catal Today 77:79–88
27. Kusche M, Enzenberger F, Bajus S, Niedermeyer H, Bosmann A, Kaftan A, Laurin M, Libuda J, Wasserscheid P (2013) Enhanced activity and selectivity in catalytic methanol steam reforming by basic alkali metal salt coatings. Angew Chem Int Ed 52:5028–5032
28. Nielsen M, Alberico E, Baumann W, Drexler HJ, Junge H, Gladiali S, Beller M (2013) Low-temperature aqueous-phase methanol dehydrogenation to hydrogen and carbon dioxide. Nature 495:85–89
29. Yang LC, Ishida T, Yamakawa T, Shinoda S (1996) Mechanistic study on dehydrogenation of methanol with $[RuCl_2(PR_3)_3]$-type catalyst in homogeneous solutions. J Mol Catal A Chem 108:87–93
30. Rodríguez-Lugo RE, Trincado M, Vogt M, Tewes F, Santiso-Quinones G, Grutzmacher H (2013) A novel liquid organic hydrogen carrier system based on catalytic peptide formation and hydrogenation. Nat Chem 5:342–347
31. Charman HB (1970) Hydride transfer reactions catalysed by rhodium–tin complexes. J Chem Soc B Phys Org 584–587. doi:10.1039/J29700000584
32. Nadeem MA, Connelly KA, Idriss H (2012) The photoreaction of TiO_2 and Au/TiO_2 single crystal and powder with organic adsorbates. Int J Nanotechnol 9:121–162
33. Nielsen M, Kammer A, Cozzula D, Junge H, Gladiali S, Beller M (2011) Efficient hydrogen production from alcohols under mild reaction conditions. Angew Chem Int Ed 50:9593–9597
34. Joo F (2008) Breakthroughs in hydrogen storage—formic acid as a sustainable storage material for hydrogen. ChemSusChem 1:805–808
35. Moret S, Dyson PJ, Laurenczy G (2014) Direct synthesis of formic acid from carbon dioxide by hydrogenation in acidic media. Nat Commun 5:4017–4023
36. Loges B, Boddien A, Gärtner F, Junge H, Beller M (2010) Catalytic generation of hydrogen from formic acid and its derivatives useful hydrogen. Top Catal 53:902–914
37. Loges B, Boddien A, Junge H, Beller M (2008) Controlled generation of hydrogen from formic acid amine adducts at room temperature and application in H_2/O_2 fuel cells. Angew Chem Int Ed 47:3962–3965
38. Junge H, Boddien A, Capitta F, Loges B, Noyes JR, Gladiali S, Beller M (2009) Improved hydrogen generation from formic acid. Tetrahedron Lett 50:1603–1606
39. Loges B, Boddien A, Junge H, Noyes JR, Baumann W, Beller M (2009) Hydrogen generation: catalytic acceleration and control by light. Chem Commun 28:4185–4187
40. Morris DJ, Clarkson GJ, Wills M (2009) Insights into hydrogen generation from formic acid using ruthenium complexes. Organometallics 28:4133–4140
41. Fukuzumi S, Kobayashi T, Suenobu T (2010) Unusually large tunneling effect on highly efficient generation of hydrogen and hydrogen isotopes in pH-selective decomposition of formic acid catalyzed by a heterodinuclear iridium–ruthenium complex in water. J Am Chem Soc 134:1496–1497
42. Maenaka Y, Suenobu T, Fukuzumi S (2012) Catalytic interconversion between hydrogen and formic acid at ambient temperature and pressure. Energy Environ Sci 5:7360–7367
43. Boddien A, Loges B, Junge H, Beller M (2008) Hydrogen generation at ambient conditions: application in fuel cells. ChemSusChem 1:751–758
44. Grasemann M, Laurenczy G (2012) Formic acid as a hydrogen source—recent developments and future trends. Energy Environ Sci 5:8171–8181
45. Boddien A, Junge H (2011) Catalysis: acidic ideas for hydrogen storage. Nature Nanotech 6:265–266
46. Solymosi F, Koós Á, Liliom N, Ugrai I (2011) Production of CO-free H_2 from formic acid. A comparative study of the catalytic behavior of Pt metals on a carbon support. J Catal 279:213–219
47. Bulushev DA, Beloshapkin S, Ross JRH (2010) Hydrogen from formic acid decomposition over Pd and Au catalysts. Catal Today 154:7–12
48. Eley DD, Luetic P (1957) The formic acid decomposition on palladium–gold alloys. Faraday Soc 53:1483–1487
49. Williams R, Crandall RS, Bloom A (1978) Use of carbon dioxide in energy storage. Appl Phys Lett 33:381–383
50. Mori K, Dojo M, Yamashita H (2013) Pd and Pd–Ag nanoparticles within a macroreticular basic resin: an efficient catalyst for hydrogen production from formic acid decomposition. ACS Catal 3:1114–1119
51. Zhou X, Huang Y, Xing W, Liu C, Liao J, Lu T (2008) High-quality hydrogen from the catalyzed decomposition of formic acid by Pd–Au/C and Pd–Ag/C. Chem Commun 30:3540–3542
52. Hu C, Pulleri JK, Ting SW, Chan KY (2014) Activity of Pd/C for hydrogen generation in aqueous formic acid solution. Int J Hydrog Energy 39:381–390
53. Wang Z, Yan JM, Wang HL, Ping Y, Jiang Q (2012) Pd/C synthesized with citric acid: an efficient catalyst for hydrogen generation from formic acid/sodium formate. Sci Rep 2:598–604
54. Wang X, Qi G, Tan C, Li Y, Guo J, Pang X, Zhang S (2014) Pd/C nanocatalyst with high turnover frequency for hydrogen generation from the formic acid–formate mixtures. Int J Hydrog Energy 39:837–843
55. Ojeda M, Iglesia E (2009) Formic acid dehydrogenation on Au-based catalysts at near-ambient temperatures. Angew Chem Int Ed 48:4800–4803
56. Metin O, Sun X, Sun S (2013) Monodisperse gold–palladium alloy nanoparticles and their composition-controlled catalysis in formic acid dehydrogenation under mild conditions. Nanoscale 5:910–912
57. Tedsree K, Li T, Jones S, Chan CWA, Yu KMK, Bagot PAJ, Marquis EA, Smith GDW, Tsang SCE (2011) Hydrogen production from formic acid decomposition at room temperature using a Ag–Pd core–shell nanocatalyst. Nat Nanotechnol 6:302–307
58. Zhang S, Metin O, Su D, Sun SH (2013) Monodisperse AgPd alloy nanoparticles and their superior catalysis for the dehydrogenation of formic acid. Angew Chem Int Ed 52:3681–3684
59. Bulut A, Yurderi M, Karatas Y, Zahmakiran M, Kivrak H, Gulcan M, Kaya M (2015) Pd-MnO_x nanoparticles dispersed on amine-grafted silica: highly efficient nanocatalyst for hydrogen production from additive-free dehydrogenation of formic acid under mild conditions. Appl Catal B 164:324–333
60. Zhu QL, Tsumori N, Xu Q (2014) Sodium hydroxide-assisted growth of uniform Pd nanoparticles on nanoporous carbon MSC-30 for efficient and complete dehydrogenation of formic acid under ambient conditions. Chem Sci 5:195–199

61. Bi QY, Du XL, Liu Y, Cao MY, He HY, Fan KN (2012) Efficient subnanometric gold-catalyzed hydrogen generation via formic acid decomposition under ambient conditions. J Am Chem Soc 134:8926–8933
62. Ping Y, Yan JM, Wang ZL, Wang HL, Jiang Q (2013) $Ag_{0.1}$-$Pd_{0.9}$/,GO: an efficient catalyst for hydrogen generation from formic acid/sodium formate. J Mater Chem A 1:12188–12191
63. Mazumder V, Chi M, Mankin M, Liu N, Metin Y, Sun OD, More KL, Sun S (2012) A facile synthesis of MPd (M=Co, Cu) nanoparticles and their catalysis for formic acid oxidation. Nano Lett 12:1102–1106
64. Wang ZL, Yan JM, Ping Y, Wang HL, Zheng WT, Jiang Q (2013) An Efficient CoAuPd/C Catalyst for hydrogen generation from formic acid at room temperature. Angew Chem Int Ed 52:4406–4409
65. Wang ZL, Ping Y, Yan JM, Wang HL, Jiang Q (2014) Hydrogen generation from formic acid decomposition at room temperature using a NiAuPd alloy nanocatalyst. Int J Hydrog Energy 39:4850–4856
66. Qin YL, Wang J, Meng FZ, Wang LM, Zhang XB (2013) Efficient PdNi and PdNi@Pd-catalyzed hydrogen generation via formic acid decomposition at room temperature. Chem Commun 49:10028–10030